



Transportation Research Division



Technical Report 14-15

Manning's Roughness Coefficient for Buried Composite Arch Bridges

Technical Report Documentation Page

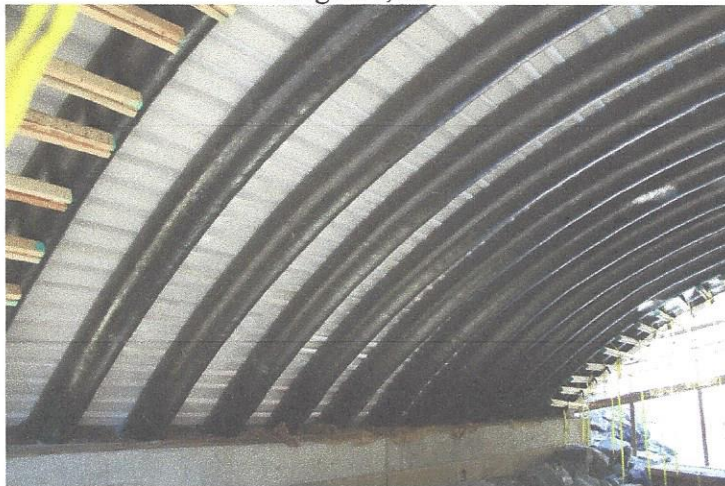
1. Report No. ME 14-15	2.	3. Recipient's Accession No.	
4. Title and Subtitle Manning's Roughness Coefficient for Buried Composite Arch Bridges		5. Report Date August 2014	
		6.	
7. Author(s) Lingqiang Yang, Ph.D Qingping Zou, Ph.D		8. Performing Organization Report No. 13-39-1023I	
9. Performing Organization Name and Address University of Maine		10. Project/Task/Work Unit No. Project 17891.00	
		11. Contract © or Grant (G) No. Contract # 20111223*2878	
12. Sponsoring Organization Name and Address Maine Department of Transportation 16 State House Station Augusta, Maine 04333		13. Type of Report and Period Covered	
		14. Sponsoring Agency Code	
15. Supplementary Notes			
16. Abstract (Limit 200 words)			
<p>This report includes fulfillment of Task 9 of a multi-task contract to further enhance concrete filled FRP tubes, or the Bridge in a Backpack. Task 9 investigates the interaction of water flow under the bridge with the tubes and decking and recommends Manning's roughness coefficients for water flow under the composite backpack bridge system.</p> <p>There are three flow regimes and each has a different resistance relationship. Quasi-smooth flow occurs only when there are depressions or when roughness elements are spaced very close. Hyper-turbulent flow occurs when roughness elements are sufficiently close so each element is in the wake of the previous element and rough surface vortices are the primary source of the overall friction drag. Isolated roughness flow occurs when roughness spacing is large and overall resistance is due to drag on the decking surface and form drag on the arches. Due to the large sizes of the tubes and tube spacing, the conventional method of computing roughness coefficient using the formula for rough pipe is not applicable here. Instead, we have to use a more complex procedure to calculate the roughness coefficient using different formula for different flow regimes described above.</p> <p>In this report, Manning's roughness coefficients are provided when the flow is perpendicular to the bridge and when the angle between flow and the bridge is 45 and 30 degrees (Appendix 1). Depending on the arch radius and tube size and spacing, Manning's roughness coefficient of the bridge ranges from 0.016 to 0.045, which is significantly larger than that for smooth concrete ($n=0.012$), due to the large tubes underneath the bridge. These results are important findings and should be incorporated in a hydraulic model such as HECRAS to more accurately predict water flows and backwater profiles at the FRP tubular bridge.</p>			
17. Document Analysis/Descriptors Concrete filled fiber reinforced polymer tubes, arch bridge, Hydraulics, roughness, mannings n		18. Availability Statement	
19. Security Class (this report)	20. Security Class (this page)	21. No. of Pages 41	22. Price

Manning's Roughness Coefficient for Buried Composite Arch Bridges

Advanced Structures and Composites Center Report Number: 13-39-1023I

Prepared for: Dale Peabody, Transportation Research Engineer
Maine Department of Transportation
16 State House Station
Augusta, Maine 04333-0016
(207) 624-3305

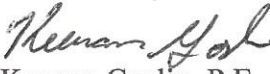
August 1, 2014



Prepared by:

Lingqiang Yang Ph.D.
Visiting Research Professor
Qingping Zou, Ph.D.
Assistant Professor of Civil Engineering

Reviewed by:


Keenan Goslin, P.E.
Structural Engineer

This report shall not be reproduced, except in full, without the written approval of Advanced Structures and Composites Center.

*An ISO 17025 accredited testing laboratory
Accredited by international Accreditation Service*



Advanced Structures and Composites Center
35 Flagstaff Rd
University of Maine
Orono, ME 04469

Telephone: 207-581-2123
FAX: 207-581-2074
composites@umit.maine.edu
www.composites.umaine.edu

EXECUTIVE SUMMARY

The Buried Composite Arch Bridge is a lightweight, corrosion resistant system for short to medium span bridge construction using FRP composite arch tubes that act as reinforcement and formwork for cast-in-place concrete (Dagher et al 2012 [1]). This study investigates the interaction of wale flow under the bridge with the tubes and decking, and recommend Manning's roughness coefficient for water flow under the composite backpack bridge system.

There are three flow regimes and each has a different resistance relationship. Quasi-smooth flow occurs only when there are depressions or when roughness elements are spaced very close. Hyper-turbulent flow occurs when roughness elements are sufficiently close so each element is in the wake of the previous element and rough surface vortices are the primary source of the overall friction drag. Isolated roughness flow occurs when roughness spacing is large and overall resistance is due to drag on the decking surface plus form drag on the arches. Due to the large size of the tubes and tube spacing, the conventional method of computing roughness coefficient using the formula for rough pipe is not applicable here. Instead, we have to use a more complex procedure to calculate the roughness coefficient using different formula for different flow regimes described above.

In this report, Manning's roughness coefficients are provided when the flow is perpendicular to bridge and when the angle between flow and bridge is 45 and 30 degrees (Appendix 1). Depending on the arch radius and tube size and spacing, Manning's roughness coefficient of the bridge ranges from 0.016 to 0.045, which is significantly larger than that for smooth concrete ($n=0.012$), due to the large tubes underneath the bridge. These results are important findings and should be incorporated in a hydraulic model such as HECRAS to more accurately predict water flows and backwater profile at the FRP tubular bridge.

TABLE OF CONTENTS

EXECUTIVE SUMMARY..... 1

1. INTRODUCTION..... 4

2. OBJECTIVE..... 6

3. METHODS..... 7

 3.1 Isolated-roughness flow..... 9

 3.2 Hyperturbulent flow..... 11

 3.3 Bridge geometry..... 13

4. RESULTS..... 16

 4.1 Relation of Manning’s n to tube diameter and tube spacing for the arch radius
 of 20.22 ft..... 17

 4.2 Relation of Manning’s n to tube diameter and tube spacing for the arch radius
 of 23.46 ft..... 20

 4.3 Relation of Manning’s n to tube diameter and tube spacing for the arch radius
 of 67.87 ft..... 20

 4.4 Relation Manning’s n to arch radius R..... 20

 4.5 Skewed bridge..... 22

5. CONCLUSIONS..... 34

6. REFERENCES..... 35

APPENDIX 1. Table of roughness coefficient (manning’s n)..... 34

APPENDIX 2. Feasibility study of physical test in UMaine flume..... 37

1. INTRODUCTION

The hybrid composite bridge system is a lightweight, corrosion resistant system for short to medium span bridge construction using FRP composite arch tubes that act as reinforcement and formwork for cast-in-place concrete [1]. Figure 1 and Figure 2 show the tubular arch structure during construction.

Presently hydraulic modeling and predictions of water flowing under the system are done using traditional tools for uniform smooth concrete arch structures. Recent storm water events have shown that better inputs for hydraulic modeling may be required to more accurately predict water flows under FRP tubular arch bridges. This study will investigate the interaction of flow under the bridge with the tubes and decking, and recommend Manning's roughness coefficient for water flow under the buried composite arch bridge system.

Determination of roughness coefficient and water resistance is a classic topic. Significant work was done in the 1950's. Recently there are a fewer studies. In 1989, Stephen T. Maynard [4] published riprap's design method, in which the Manning's coefficient is obtained by particle-size analysis. This method is not suitable for this technology. He and C. Ariyaratne (2011)[5], Stefano Pagliara (2011)[6], and B. Mottahed (1996)[7] studied similar engineering problems, but no calculation of Manning's n or relative roughness was presented in their papers. Unlined rock tunnels are similar to this technology. In reference [8,9], empirical formulas were proposed to calculate the roughness coefficient. Four general approaches can be taken for selecting the n value for uniform flow: (1) looking up tables or photographs of channel reaches for typical n values which can be used to estimate n for a different reach with recognizably similar characteristics; (2) measuring friction slopes, discharges and some cross-sections, which is both time consuming and very expensive in practice; (3) adopting empirical formulas to estimate the values of roughness based on the particle size distribution curve of channel bed material; or (4) adopting empirical formulas to estimate the values of roughness based on friction slope or water surface slope.

The large surface roughness of the buried hybrid composite arch bridge, due to the large tubes, introduces larger friction and drag to the river flow than normal culverts. The flow is different from uniform flow. This creates a non-uniform, tumbling flow. It is more difficult to determine Manning's number, n , for this type of flow.



Figure 1. One of the construction sites

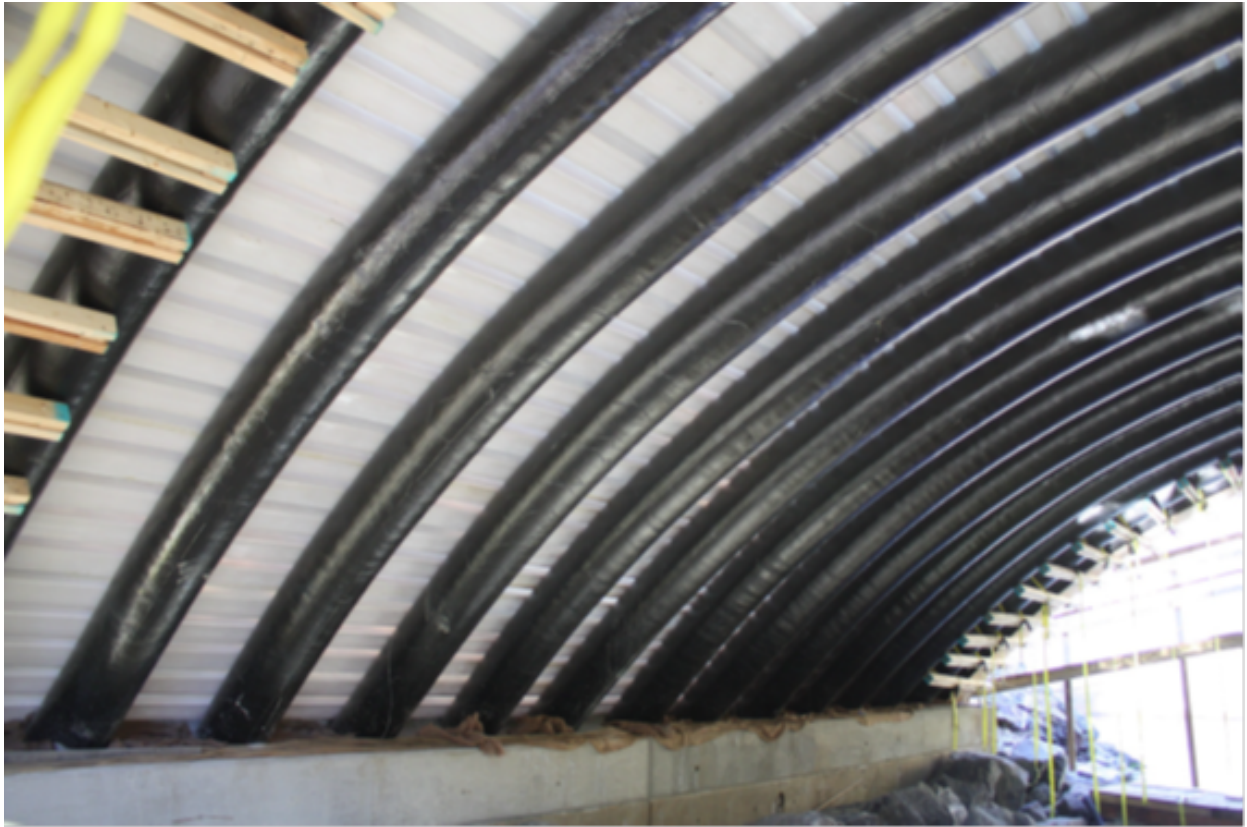


Figure 2. A view from the foundation

2. OBJECTIVE

The objective of this work is to investigate the Manning's n value as an input parameter for HEC-RAS [10], as in Figure 3 to examine the hydraulic characteristic of the river with this arch bridge technology coefficient, such as backwater.

3. METHODS

The bridge is treated as an open channel, and the diameter is varied to obtain vertical clearance for free surface flow as shown in Figure 4. Wiggery and Erfle [11] show that tumbling flow is uniform flow in a cyclical sense, with the same patterns of depth and velocity repeated at each roughness element. It is not necessary to cover the entire length of the culvert with roughness elements to get outlet velocity control. Five rows of roughness elements are sufficient to establish the cyclical uniform flow pattern.

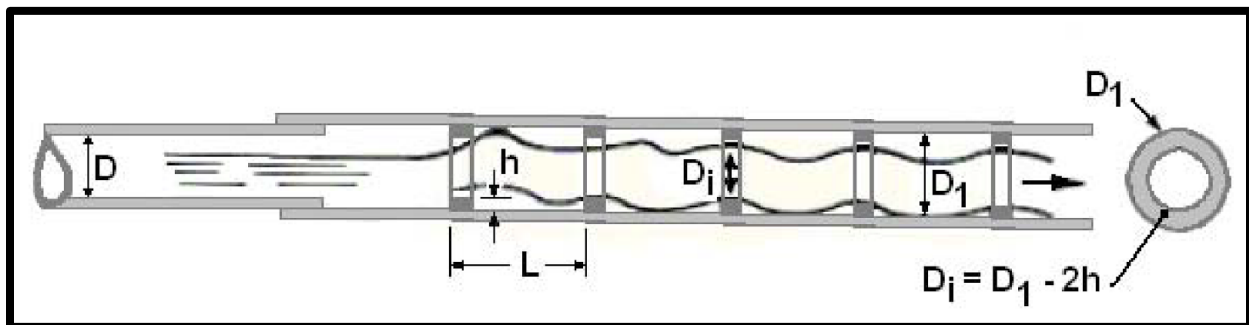


Figure 4: Definition sketch for flow in circular culverts.

Morris (1963) [12] studied all pertinent rough pipe flow data available and concluded that there are three flow regimes and each has a different resistance relationship. Conceptually, the description of these regimes also applies to box culverts. The three regimes illustrated in Figure 5 are:

- a. Quasi-smooth flow: Occurs only when there are depressions or when roughness elements are spaced very close (L/h approximately smaller or equal to 2).
- b. Hyper-turbulent flow: Occurs when roughness elements are sufficiently close so each element is in the wake of the previous element and rough surface vortices are the primary source of the overall friction drag.

- c. Isolated roughness flow: Occurs when roughness spacing is large and overall resistance is due to drag on the culvert surface plus form drag on the roughness elements.

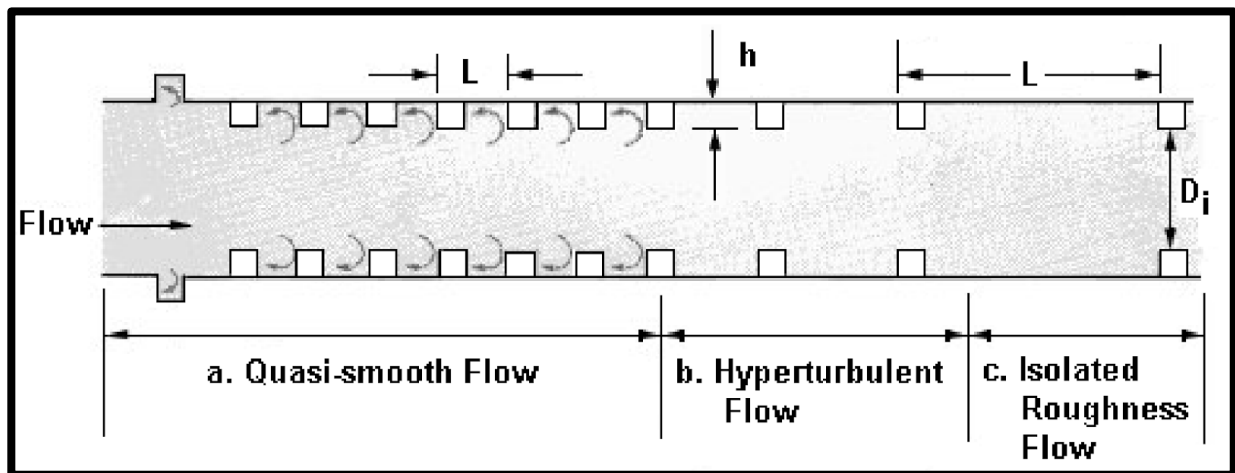


Figure 5: Flow regimes in rough pipes.

Wiggert and Erfle (1971) [13] studied the effectiveness of roughness rings as energy dissipaters in circular culverts. Although their study was primarily a tumbling flow study, they observed in many tests that they could get velocity reductions greater than 50 percent without reaching the roughness level necessary for tumbling flow. They did not derive resistance equations, but they did establish approximate design limits.

From these studies, good performance of flow type was observed when h/D was 0.06 to 0.09 using five rings (See Figure 6.) Doubling the height, h_1 , of the first ring was effective in triggering full flow in the roughened zone. Adequate performance was obtained with four identical rings, but with double spacing between the first two. However, the same pipe length is involved if a constant spacing is maintained and five rings used, with the first double the height of the other four. The additional ring should help establish the assumed full flow condition. In addition, the last (downstream) ring must be located no closer than one-half the ring spacing from the end of the culvert.

Subsequent experience reported by the American Concrete Pipe Association (ACPA, 1972)[12] indicated a need to consider lower values of h/D , and to establish approximate resistance curves for evaluating a design in order to avoid installations that will propagate full flow upstream to the culvert inlet.

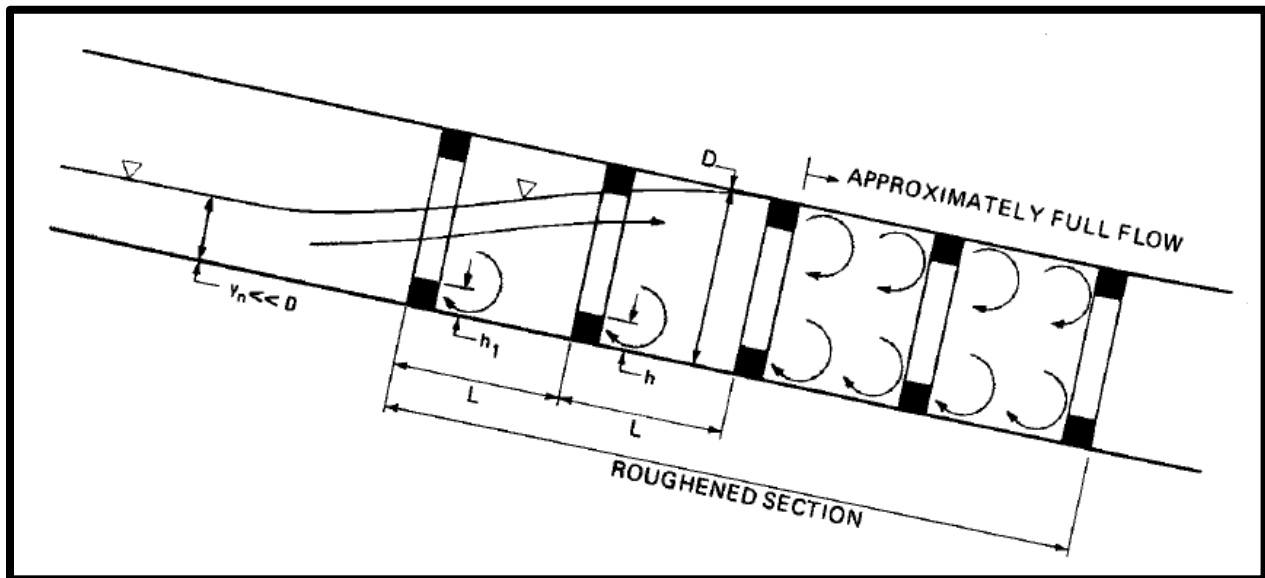


Figure 6: Conceptual sketch of roughness elements to increase resistance.

Based on experience with large elements used to force tumbling flow [12] and the work of Wiggert and Erfle (1971), five rows of roughness elements with heights ranging from 5 to 10 percent of the culvert diameter are sufficient key elements in the design of increased roughness elements is determination of the roughness regime and, subsequently, the appropriate Manning's n value. Although much of the literature relevant to large roughness elements in circular pipes represent the resistance using the friction factor, " f ", all resistance equations are converted to Manning's " n " expressions for this report.

3.1 Isolated-Roughness Flow

Ordinarily smooth conduit surface is interspersed with occasional isolated roughness elements. The over-all friction factor for these surfaces will be that due to the friction drag at the laminar boundary layer plus that due to the form drag forces on the roughness elements, a phenomenon

illustrated in Figure 7. Since both skin friction and form drag are fundamentally viscous phenomena, the same general function can be used to characterize both the main difference lying in the controlling boundary geometry. Starting from the general flow equation, and eliminating extraneous forces and dimensions, gives the overall friction or resistance, f_{IR} , which is made up of two parts:

$$f_{IR} = f_s + f_d \quad (1)$$

where,

f_s = friction on the culvert surface.

f_d = friction due to form drag on the roughness elements.

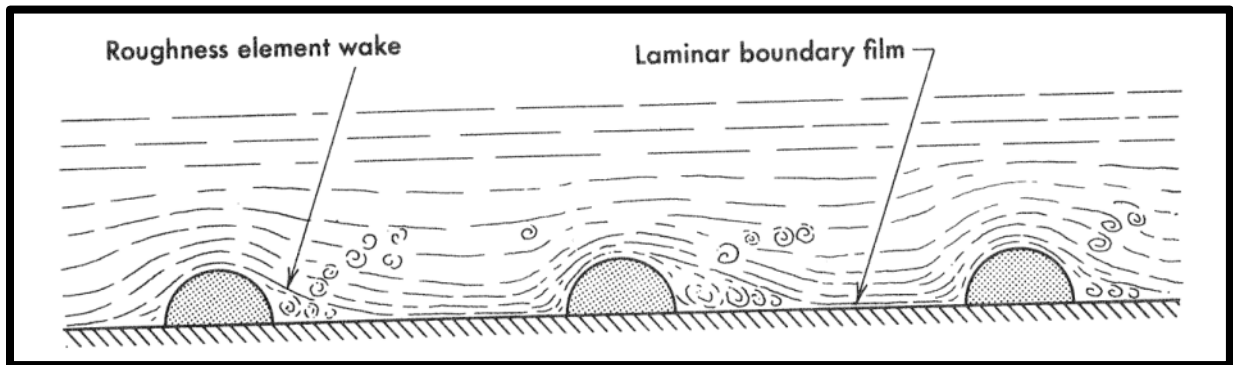


Figure 7: Isolated Roughness Flow

The friction due to form drag is a function of the drag coefficient for the particular shape, the percentage of the wetted perimeter that is roughened, the roughness dimensions and spacing and the velocity impinging on the roughness elements. Morris (1963) related the velocity to surface drag and derived the following equation:

$$f_{IR} = f_s \left(1 + 67.2 C_D \left(\frac{L_r}{P} \right) \left(\frac{h}{r_i} \right) \left(\frac{r_i}{L} \right) \right) \quad (2)$$

where, C_D = drag coefficient for the roughness shape. L_r/P is the ratio of total peripheral length of roughness elements to total wetted perimeter. r_i equals pipe radius based on the inside

diameter of roughness rings measured from crest to crest. L_r may be less than P to facilitate constructability of the rings or to permit a low flow opening at the bottom of the ring.

Throughout Morris' work, he used measurements from crest to crest of a roughness element ring as the effective diameter, D_i . The following expressions are needed to convert the expression for roughness to Manning's n :

$$f_s = \alpha(n/D^{1/6})^2 \quad (3)$$

$$f_{IR} = \alpha(n_{IR}/D_i^{1/6})^2 \quad (4)$$

α represents a unit conversion constant equal to 124 in SI and 184 in customary units.

Equation (2) can then be converted to Manning's n :

$$n_{IR} = n\left(\frac{D_i}{D}\right)^{1/6}\left(1 + 67.2C_D\left(\frac{L_r}{P}\right)\left(\frac{h}{L}\right)\right)^{1/2} \quad (5)$$

Where, n_{IR} = overall Manning's "n" for isolated roughness flow.

Therefore, n equals Manning's "n" for the culvert surface without roughness rings which can be found easily in the textbook reference [9,12,15]. D is the nominal diameter of the culvert, m (ft)

D_i = inside diameter of roughness rings, m (ft) ($D_i = D - 2h$).

For sharp edged rectangular shapes, a constant value of 1.9 can be used for CD . For circle roughness shape, C_D is 1.2. For semi-circle, it is 0.9 [13]. It is noteworthy that the overall resistance, Manning's value, n_{IR} , decreases as the relative spacing of roughness, L/D_i , increases for this flow regime.

3.2 Hyper Turbulent Flow

If the wall roughness elements are sufficiently close together, the wake behind each may extend to or nearly to the next element. There is then essentially no part of the wall over which a laminar boundary layer exists. Furthermore the vortex generation and dissipation phenomena associated

with each wake will interfere with those at the adjacent elements, so that the individual effects are not additive as in the case of isolated roughness flow in Section 3.1.

The over-all phenomenon of wake interference results in a zone near the wall of abnormally intense turbulence and mixing. The velocity distribution will be normal in the central regions, but the average slope near the wall will be somewhat flatter than normal, indicating a higher relative degree of turbulent mixing in this zone. The type of flow is illustrated in Figure 8.

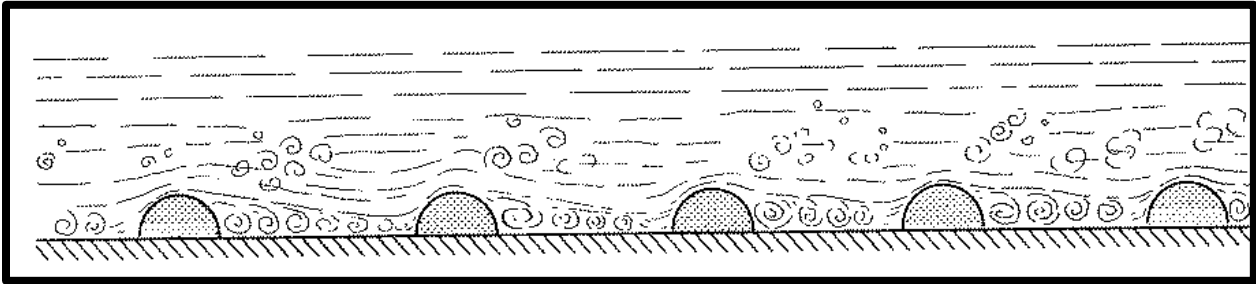


Figure 8: Hyper Turbulent Flow

The friction in this regime is independent of friction on the culvert surface:

$$f_{HT} = \left(\frac{1}{2 \log\left(\frac{r_i}{L}\right) + 1.75 + \phi} \right)^2 \quad (6)$$

where,

f_{HT} equals overall friction for hyper-turbulent flow, and ϕ is the function of Reynolds number, element shape, and relative spacing.

If the flow is not laminar flow, it can be neglected. Substituting the following expression:

$$f_{HT} = \alpha \left(\frac{n_{HT}}{D_i^{1/6}} \right)^2$$

Equation (6) can then be converted to Manning's n :

$$n_{HT} = \frac{\alpha D_i^{1/6}}{2 \log\left(\frac{r_i}{L}\right) + 1.75} \quad (7)$$

where, n_{HT} = Manning's n for hyper-turbulent flow, and α equals unit conversion constant, 0.0898 (SI) and 0.0737 (CU).

The effect of the roughness height, h , is included inherently in D_i . From equation (7), it can be seen that n_{HT} increases as the roughness spacing increases for this flow regime. This trend is opposite of that for isolated-roughness flow.

3.3. Bridge Geometry

Figure 9 shows a typical bridge geometry. Figure 10 and Figure 11 show a representative range of bridge span and tube spacing.

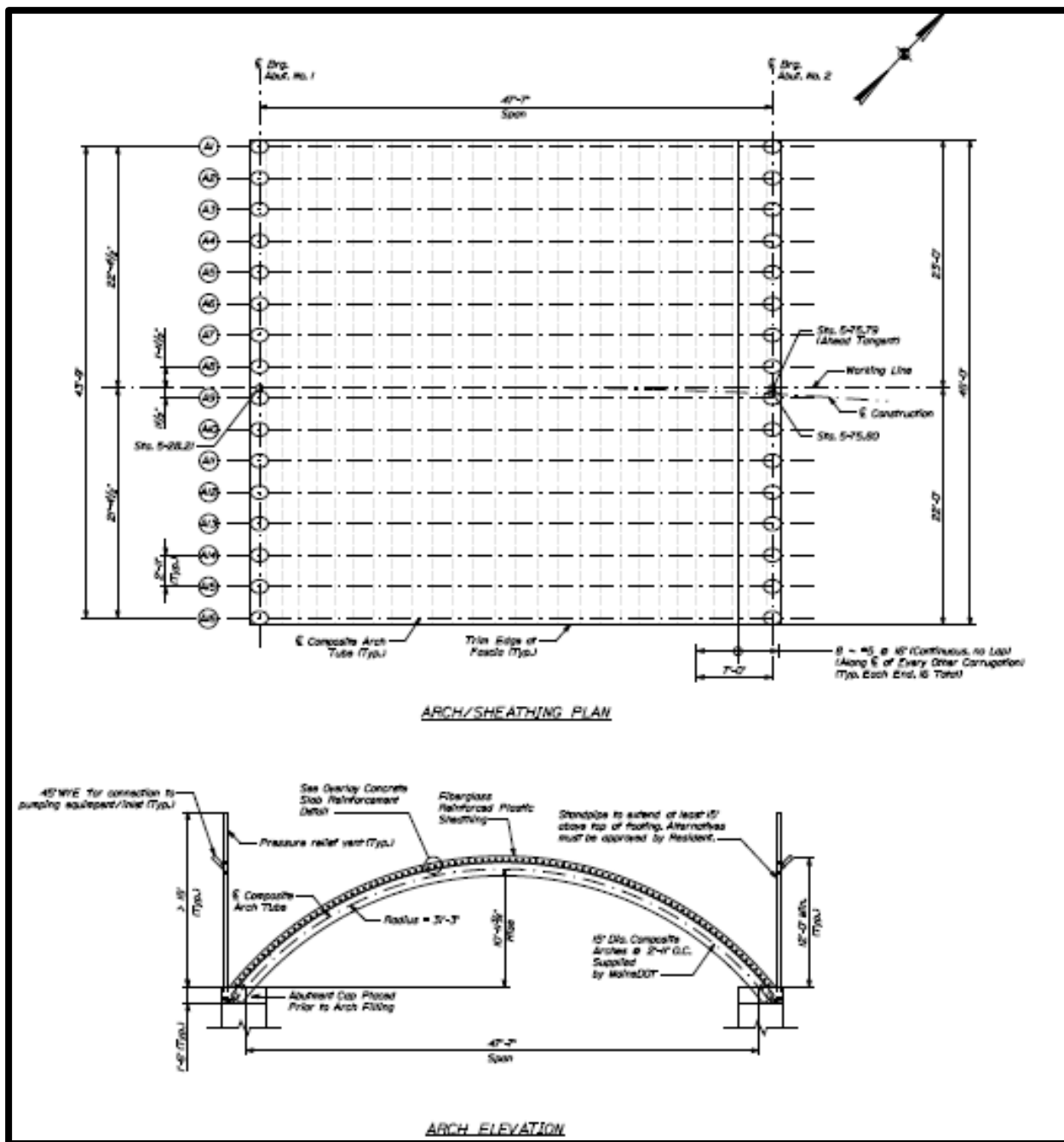


Figure 9: Bridge Geometry

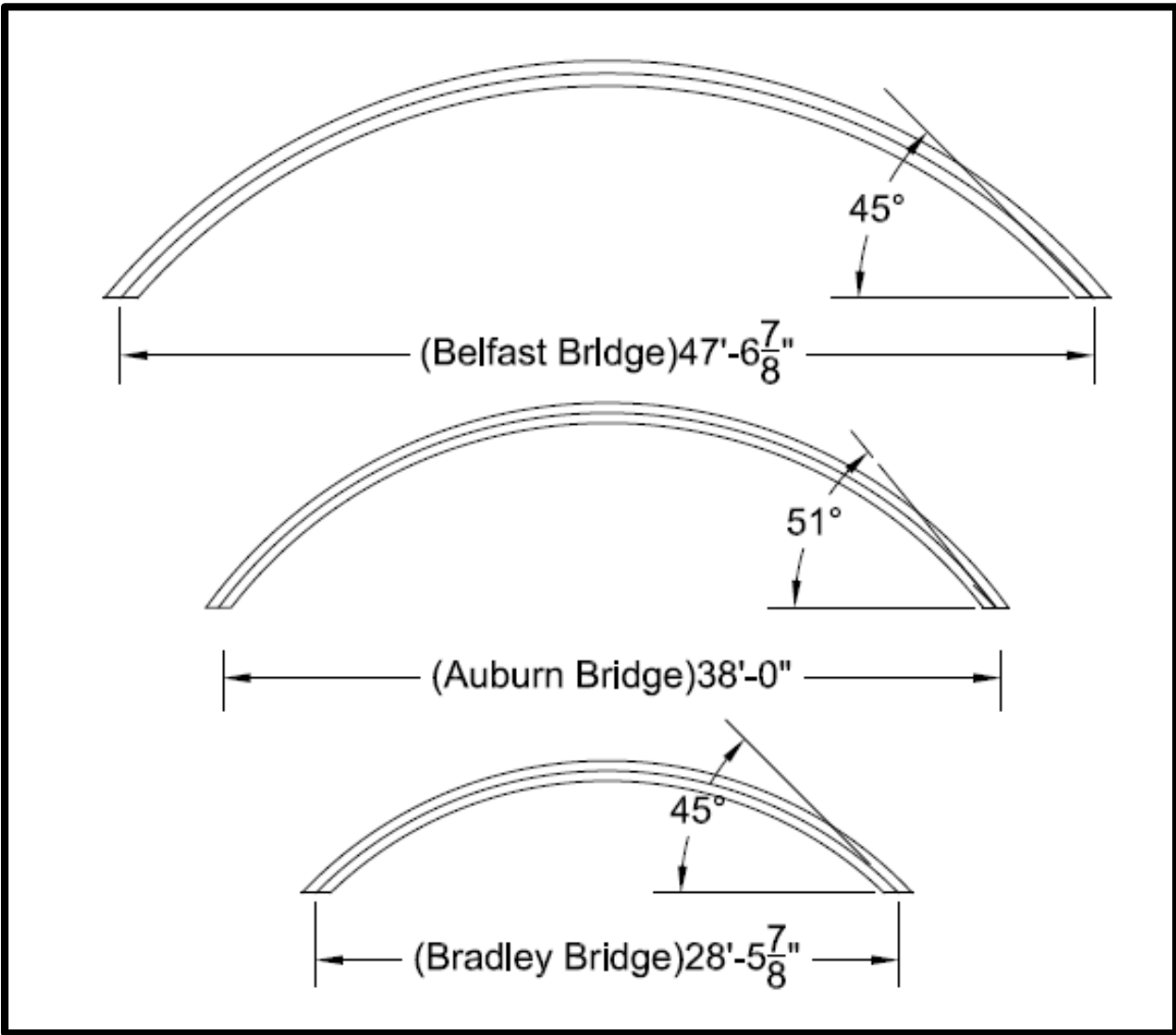


Figure 10: Range of Bridge Span

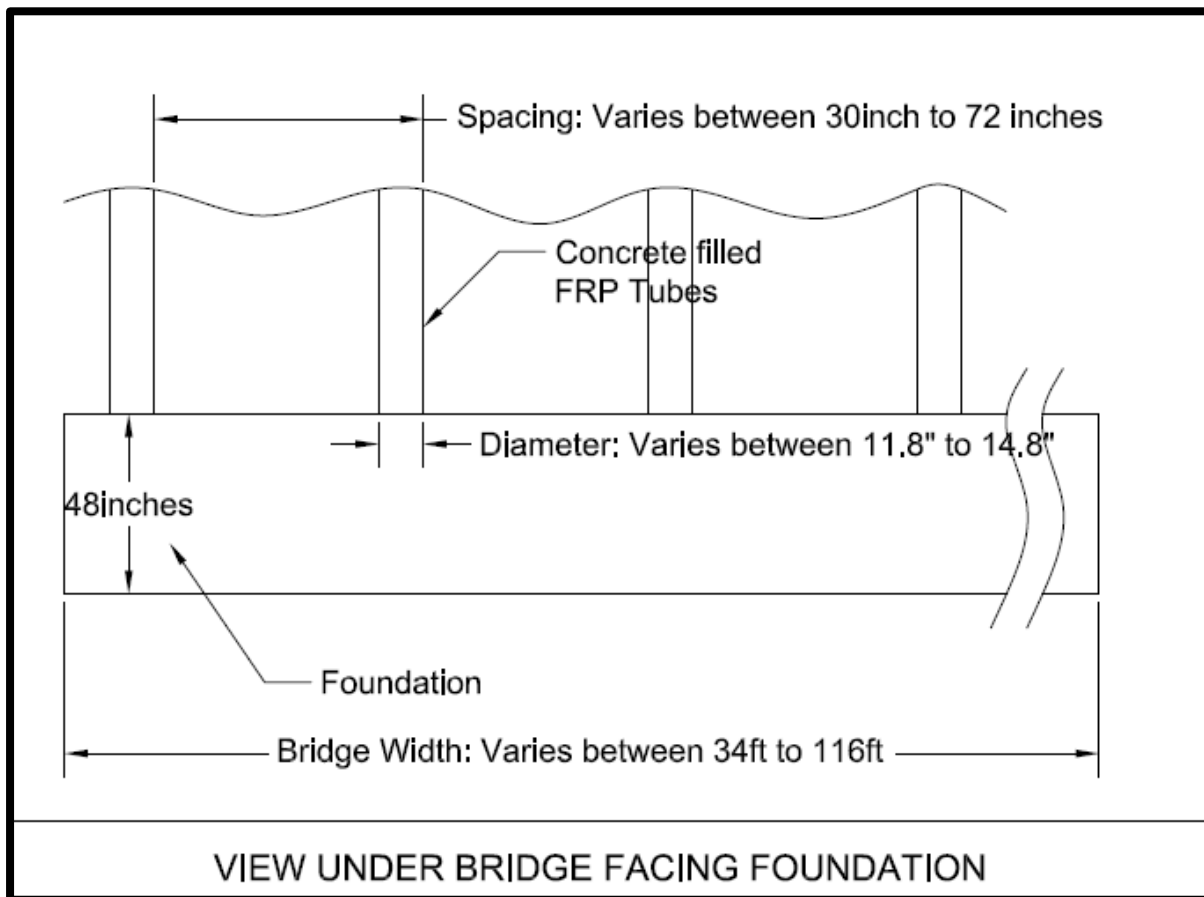


Figure 11: Range of tube spacings, diameter, and bridge width.

4. RESULTS

There are 3 factors affecting Manning's n that were investigated: the first is the radius of arch R ; the second is the tube diameter d , and the third is the spacing of tubes, L .

4.1 Relation of Manning's n to tube diameter and tube spacing

Relation of Manning's n to tube diameter and tube spacing for a radius of arch of 20.22 ft. assuming the radius of arch R is 20.22 ft. and changing the diameter of the tube and tube spacing, the calculating result of Manning's n is given in Table 1 and Figure 12.

Table 1: Manning's n (radius of arch $R = 20.22$ ft.)

<i>Tube spacing(in)</i>	<i>d=11.8in</i>	<i>12.8in</i>	<i>13.8in</i>	<i>14.8in</i>
30	0.038	0.038	0.038	0.038
36	0.040	0.040	0.040	0.040
42	0.042	0.042	0.042	0.042
48	0.043	0.043	0.044	0.044
54	0.043	0.044	0.045	0.045
60	0.041	0.042	0.044	0.045
66	0.039	0.040	0.042	0.043
72	0.037	0.039	0.040	0.041
78	0.036	0.037	0.039	0.040
84	0.035	0.036	0.037	0.039
90	0.034	0.035	0.036	0.037
96	0.033	0.034	0.035	0.036
102	0.032	0.033	0.034	0.035
108	0.031	0.032	0.033	0.034

4.2 Relation of Manning's n to tube diameter and tube spacing

Relation of Manning's n to tube diameter and tube spacing for a radius of arch of 23.46 ft. assumed the radius of arch R is 23.46 ft., the diameter of tube and tube spacing is changed. The calculating result of Manning's n is as follow Table 2 and Figure 13.

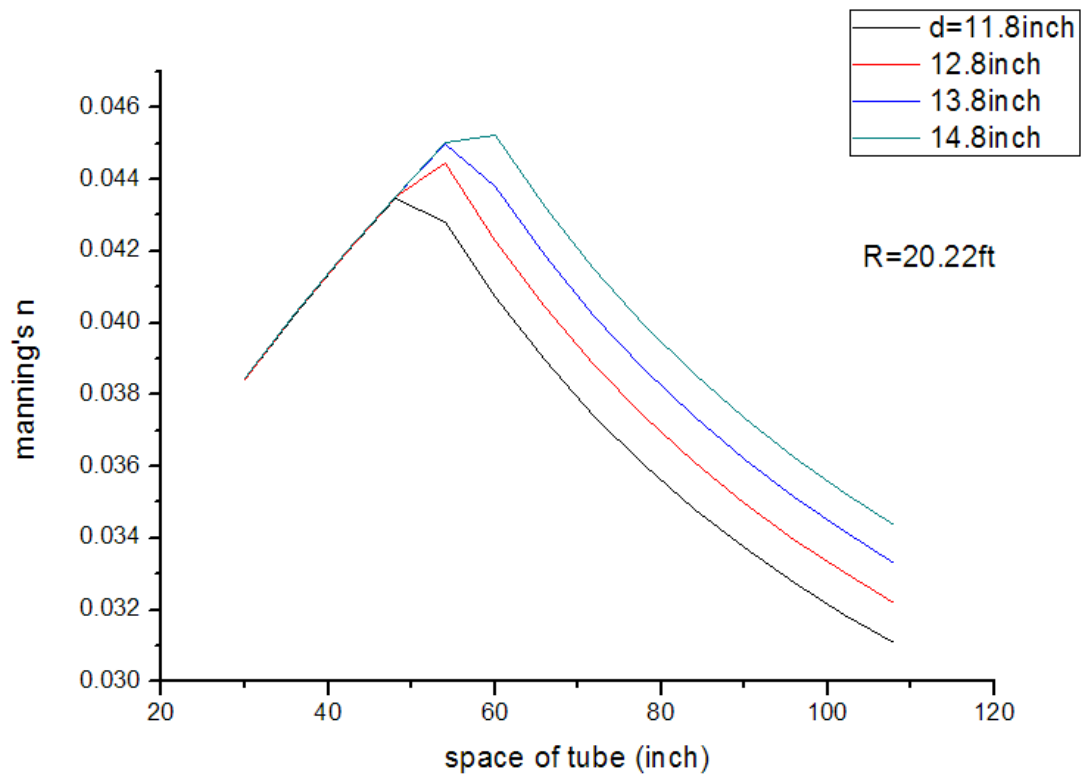


Figure12: Manning's n with a different tube diameter and tube spacing (Radius of arch: 20.22 ft.)

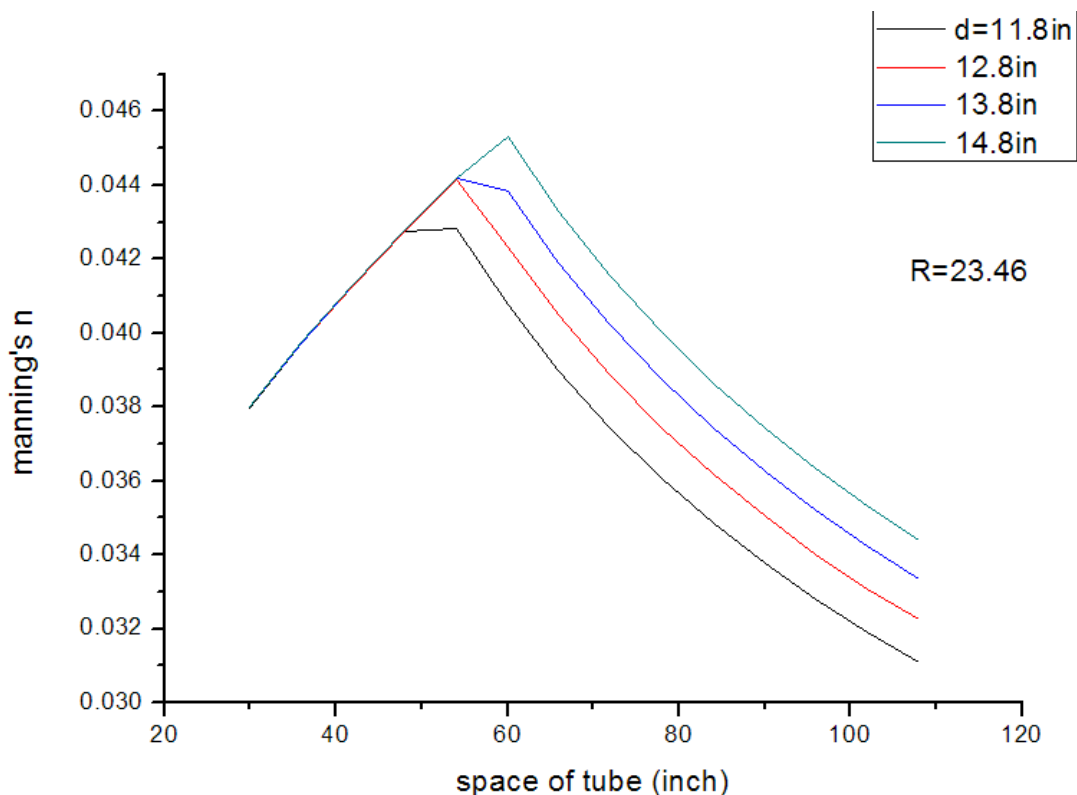


Figure 13: Manning's n with different tube diameter and tube spacing (Radius of arch: 23.46 ft.)

Table 2: Manning's n (radius of arch R = 23.46 ft.)

Spacing of tubes(in)	d=11.8in	12.8in	13.8in	14.8in
30	0.038	0.038	0.038	0.038
36	0.040	0.040	0.040	0.040
42	0.041	0.041	0.041	0.041
48	0.043	0.043	0.043	0.043
54	0.043	0.044	0.044	0.044
60	0.041	0.042	0.044	0.045
66	0.039	0.040	0.042	0.043
72	0.037	0.039	0.040	0.042
78	0.036	0.037	0.039	0.040
84	0.035	0.036	0.037	0.039
90	0.034	0.035	0.036	0.037
96	0.033	0.034	0.035	0.036

102	0.032	0.033	0.034	0.035
108	0.031	0.032	0.033	0.034

4.3. Relation of Manning’s n to tube diameter and tube spacing

Relation of Manning’s n to tube diameter and tube spacing for an arch radius of 67.87 ft. assumed the radius of arch R is 23.46 ft., the diameter of tube and tube spacing is changed. The calculating result of Manning’s n is as follow Table 3 and Figure 14.

Table 3: Manning's n (radius of arch R = 67.87 ft.)

<i>Tube spacing(in)</i>	<i>d=11.8in</i>	<i>12.8in</i>	<i>13.8in</i>	<i>14.8in</i>
30	0.036	0.036	0.036	0.036
36	0.037	0.037	0.037	0.037
42	0.039	0.039	0.039	0.039
48	0.040	0.040	0.040	0.040
54	0.041	0.041	0.041	0.041
60	0.041	0.042	0.042	0.042
66	0.039	0.041	0.042	0.043
72	0.038	0.039	0.040	0.042
78	0.036	0.038	0.039	0.040
84	0.035	0.036	0.038	0.039
90	0.034	0.035	0.036	0.038
96	0.033	0.034	0.035	0.037
102	0.032	0.033	0.034	0.036
108	0.031	0.032	0.034	0.035

4.4. Relation Manning’s n to arch radius R

The relation of Manning’s n to arch radius R is illustrated in Figure 15. It shows that when the tube spacing is small, the Manning’s n decreases with the arch radius as in line 1, 2, 3 and 4.

However, when the space of the tube is large, the Manning's n does no change with arch radius R, but the diameter of tube affect the Manning's n. A constant turning angle of the arch was held while changing R of the approximately 100 degrees.

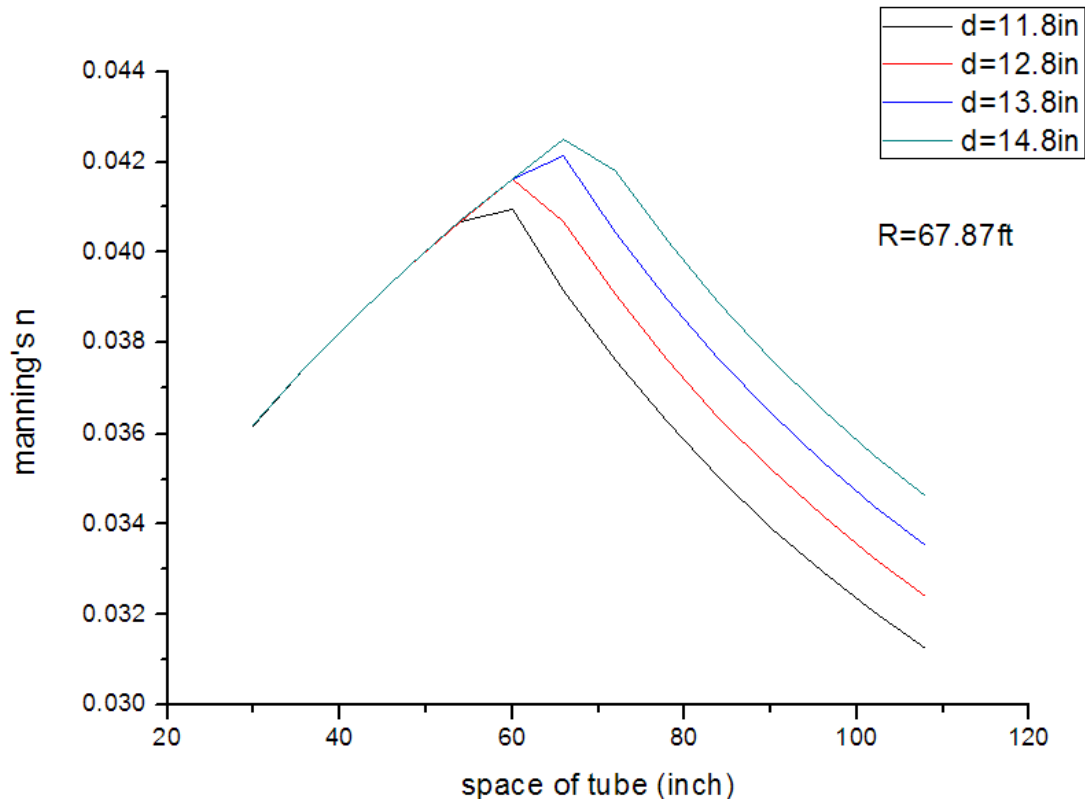


Figure 14: Manning's n with different tube diameter and tube spacing (Radius of arch: 67.87 ft.)

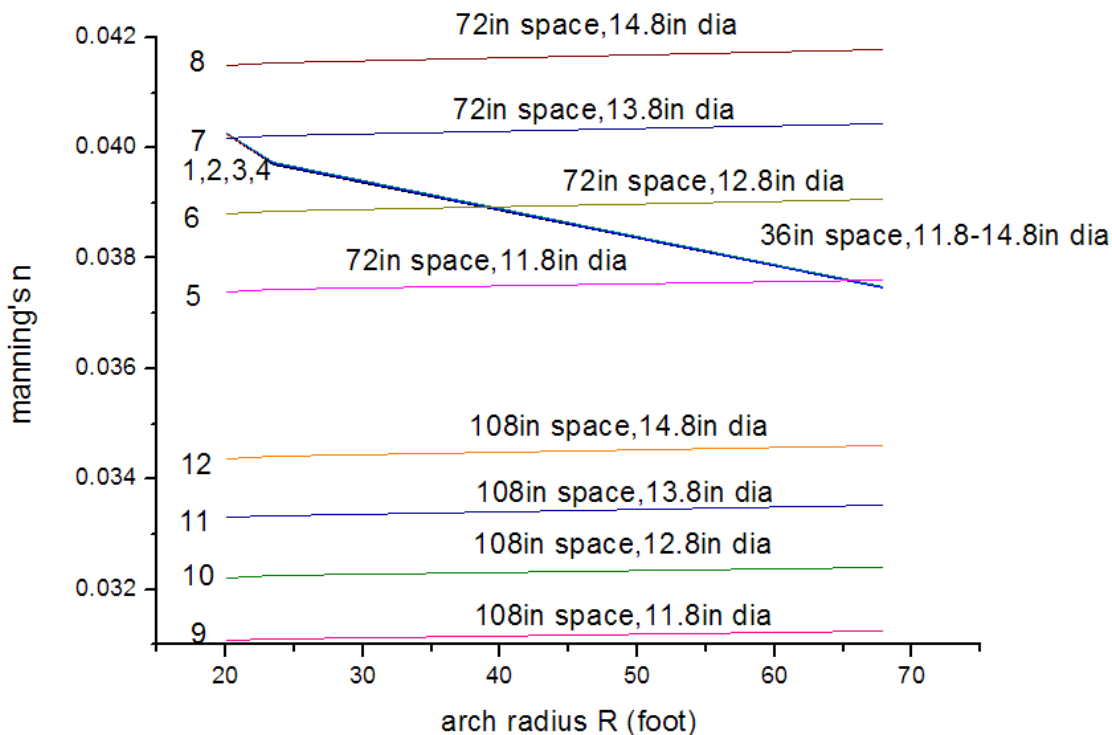


Figure 15: Manning's n with arch radius R

4.5. Skewed Bridge

In the case of skewed crossings (Figure 16), Manning's n is the same as normal crossings. According to experimental studies with yawed cylinders [16-18], the effect of the angle of attack on normal force coefficient parameter for circular cylinder is in Figure 18. The relation of Reynolds Number and $\frac{C_n}{\sin^2 \alpha}$ is given in Table 4. The relation between drag coefficient C_d and normal force coefficient C_n is:

$$C_d = \frac{C_n}{\sin^2 \alpha} \sin^3 \alpha \quad (8)$$

The relation of Reynolds Number with flow speed is in Table 5.

Table 4: The relation of Reynolds Number and $C_n/\sin^2 \alpha$

<i>Reynolds Number</i>	$\frac{V^2}{\nu}$	
$Re < 10^5$		1.2
$10^5 < Re < 4 \times 10^5$		1.2 ~0.6
$Re > 4 \times 10^5$		0.6-0.7

Table 5: The relation of Reynolds Number and flow speed.

<i>Angle of flow and bridge</i>	C_d
90°	1.2
30°	0.26
45°	0.212

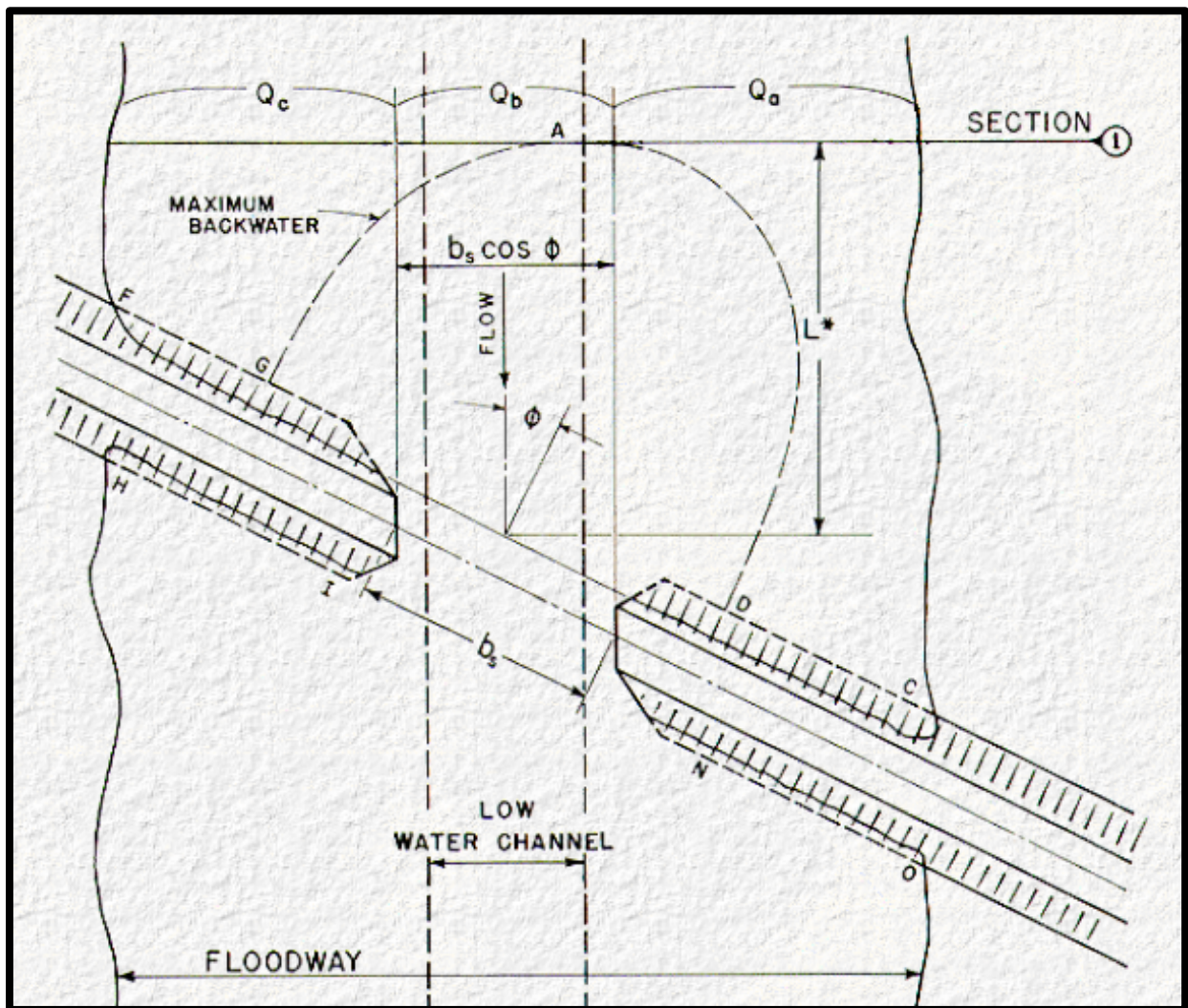


Figure 16. Skewed crossings [10]

4.5.1. Manning's n for a radius of arch of 20.22 ft., flow angle of 45°

Resulting Manning's number is given in Table 6 and assumed the radius of arch R is 20.22 ft. the diameter of tube and tube spacing is changed. The calculating result of Manning's n is as follows in Table 6 and Figure 18 where a constant radius of 20, 22 feet is held. The tube diameter and spacing are varied as shown

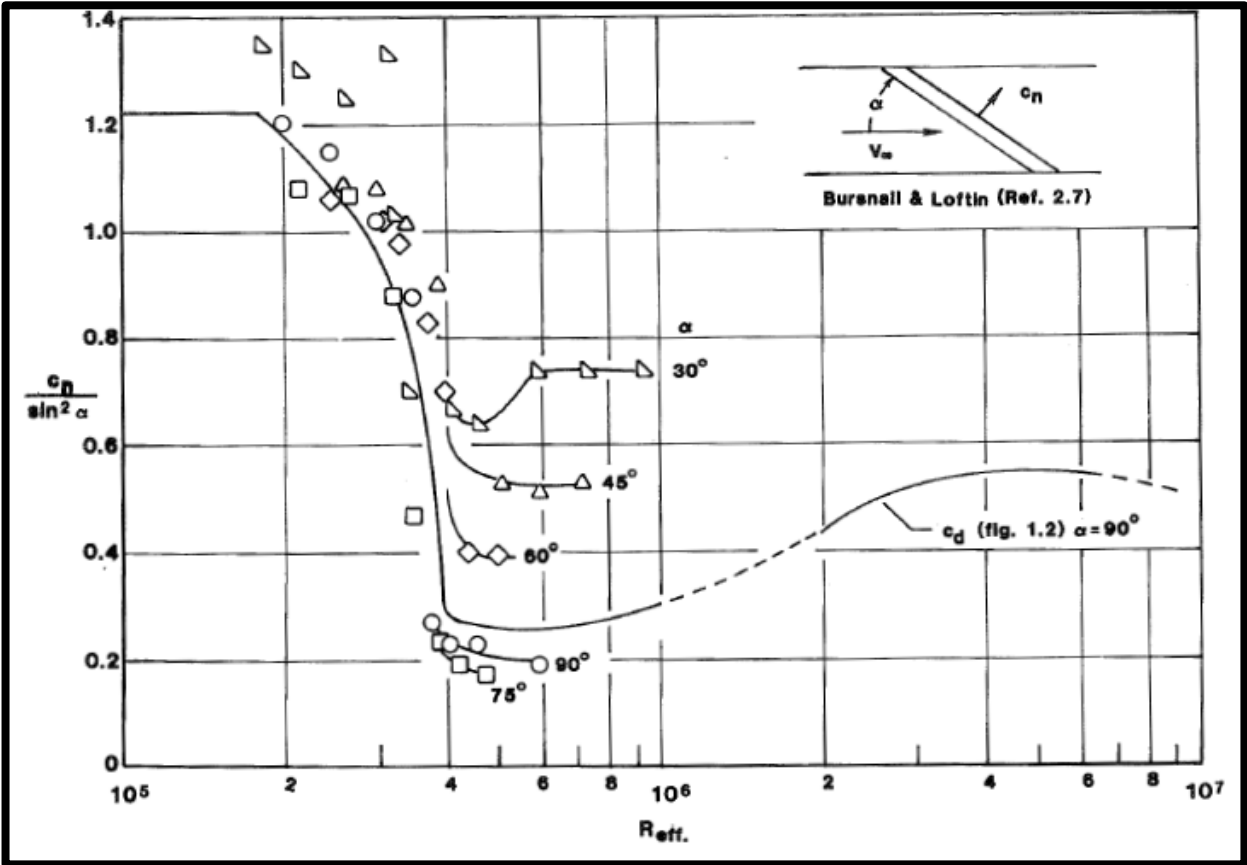


Figure 17. Effect of attack angle on normal force coefficient parameter for circular cylinder [18]

Table 6: Manning's n (radius of arch R=20.22 ft., flow angle = 45 degrees).

<i>Tube spacing at flow direction (in)</i>	<i>d=11.8in</i>	<i>12.8in</i>	<i>13.8in</i>	<i>14.8in</i>
30	0.025	0.026	0.027	0.028
36	0.024	0.024	0.025	0.026
42	0.022	0.023	0.024	0.024
48	0.021	0.022	0.022	0.023
54	0.020	0.021	0.021	0.022
60	0.019	0.020	0.020	0.021
66	0.019	0.019	0.020	0.020
72	0.018	0.019	0.019	0.020
78	0.018	0.018	0.019	0.019
84	0.017	0.018	0.018	0.019
90	0.017	0.017	0.018	0.018
96	0.016	0.017	0.017	0.018
102	0.016	0.017	0.017	0.017
108	0.016	0.016	0.017	0.017

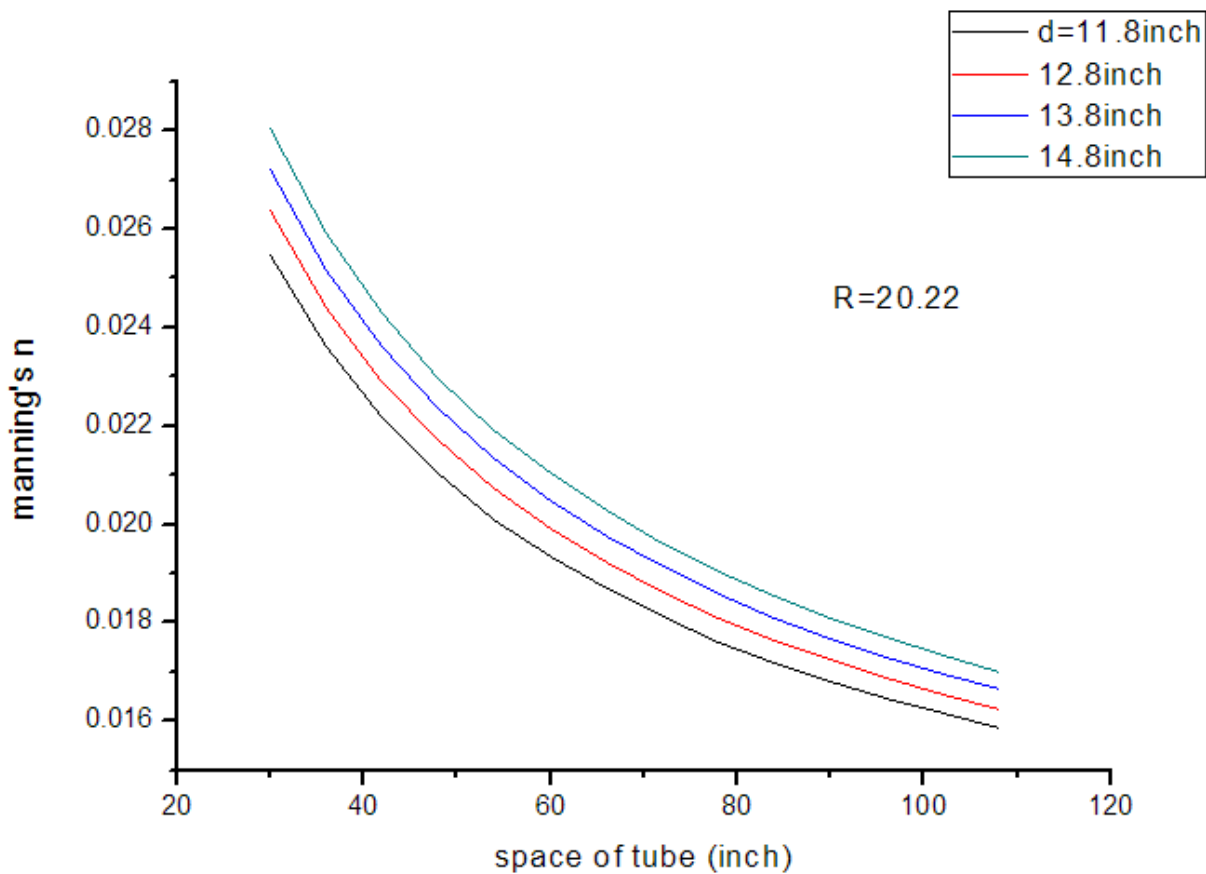


Figure 18: Manning's n with different tube diameter and tube spacing (Radius of arch: 20.22 ft., Flow angle: 45 degrees).

4.5.2. Manning's n for an arch radius of 23.46 ft., flow angle of 45°

Assumed the radius of arch R is 23.46 ft. the diameter of tube and tube spacing is changed. The calculating result of Manning's n is as follows in Table 7 and Figure 19.

Table 7: Manning's n (Radius of arch R: 23.46 ft., Flow angle: 45 degrees).

<i>Tube spacing at flow direction (in)</i>	<i>d=11.8in</i>	<i>12.8in</i>	<i>13.8in</i>	<i>14.8in</i>
30	0.026	0.026	0.027	0.028
36	0.024	0.024	0.025	0.026
42	0.022	0.023	0.024	0.024
48	0.021	0.022	0.022	0.023
54	0.020	0.021	0.021	0.022
60	0.019	0.020	0.021	0.021
66	0.019	0.019	0.020	0.020
72	0.018	0.019	0.019	0.020
78	0.018	0.018	0.019	0.019
84	0.017	0.018	0.018	0.019
90	0.017	0.017	0.018	0.018
96	0.016	0.017	0.017	0.018
102	0.016	0.017	0.017	0.017
108	0.016	0.016	0.017	0.017

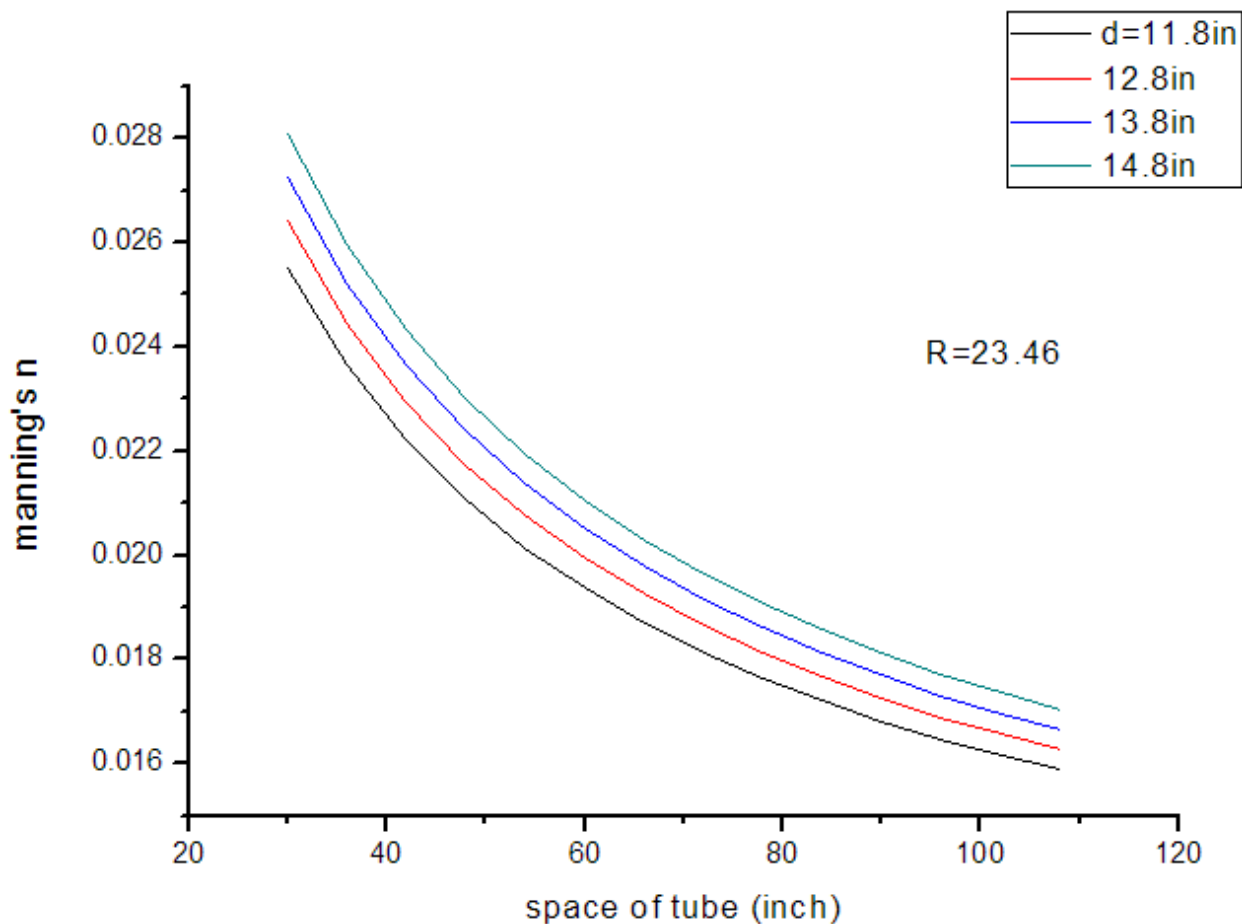


Figure 19: Manning's n with different tube diameter and tube spacing (Radius of arch: 23.46 ft., Flow angle: 45 degrees).

4.5.3. Manning's n for a arch radius of 67.87 ft, flow angle of 45°

Assumed the radius of arch R is 67.87ft., the diameter of tube and tube spacing is changed. The calculating result of Manning's n is as following Table 8 and Figure 20.

Table 8: Manning's n (Radius of arch R: 67.87 ft., Flow angle: 45 degrees).

Tube spacing at flow direction (in)	d=11.8in	12.8in	13.8in	14.8in
30	0.026	0.027	0.027	0.028
36	0.024	0.025	0.025	0.026
42	0.022	0.023	0.024	0.024
48	0.021	0.022	0.023	0.023
54	0.020	0.021	0.021	0.022
60	0.019	0.020	0.021	0.021
66	0.019	0.019	0.020	0.020
72	0.018	0.019	0.019	0.020
78	0.018	0.018	0.019	0.019
84	0.017	0.018	0.018	0.019
90	0.017	0.017	0.018	0.018
96	0.017	0.017	0.017	0.018
102	0.016	0.017	0.017	0.017
108	0.016	0.016	0.017	0.017

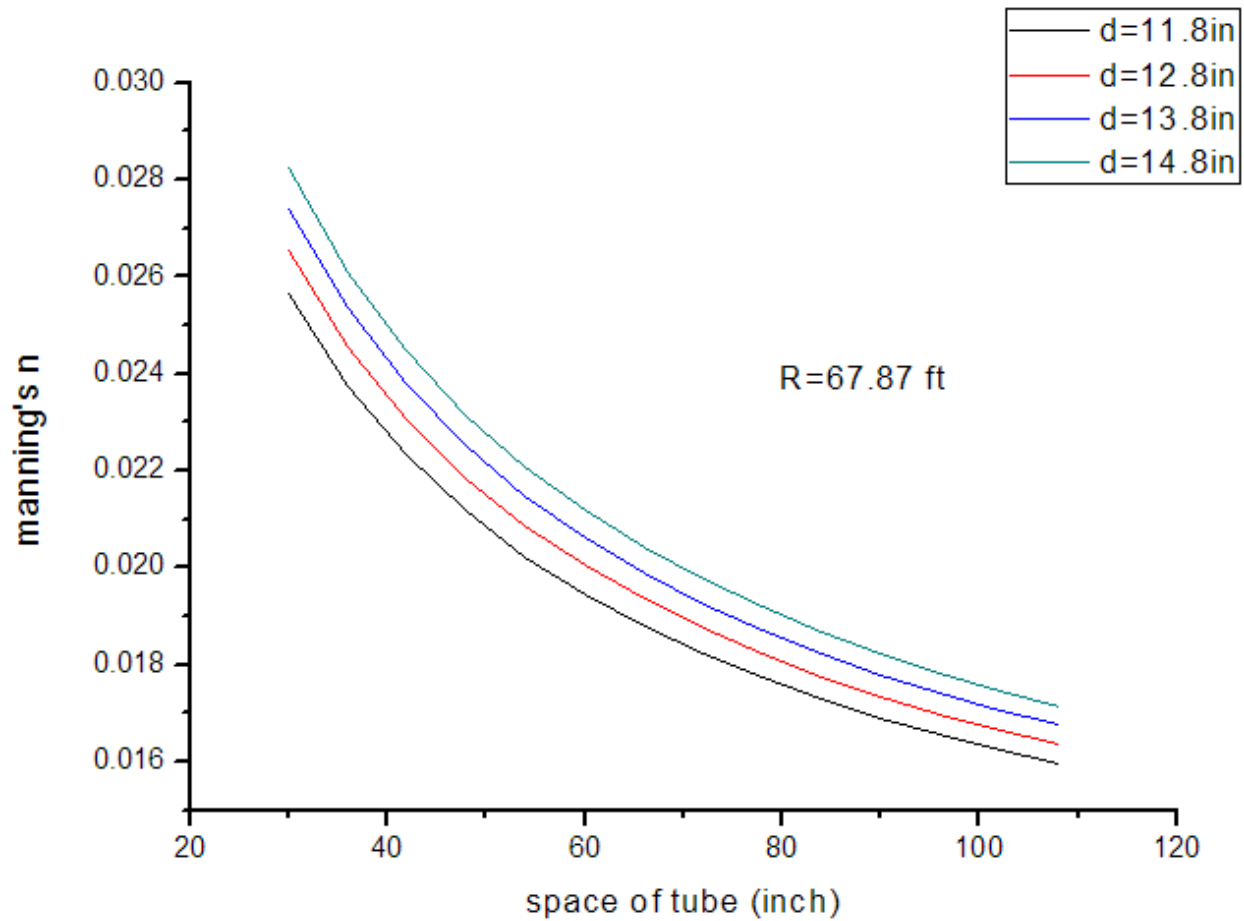


Figure 20: Manning's n with different tube diameter and tube spacing (Radius of arch: 67.87 ft., Flow angle: 45 degrees).

4.5.4. Relation of Manning's n to arch radius R

The relation of Manning's n with arch radius R is illustrated in Figure 21. It shows that Manning's n does not change with arch radius R, but the diameter of tube does affect the Manning's n. Radius is used here to vary span and rise of the arches, but the span to rise ratio is held constant in this analysis.

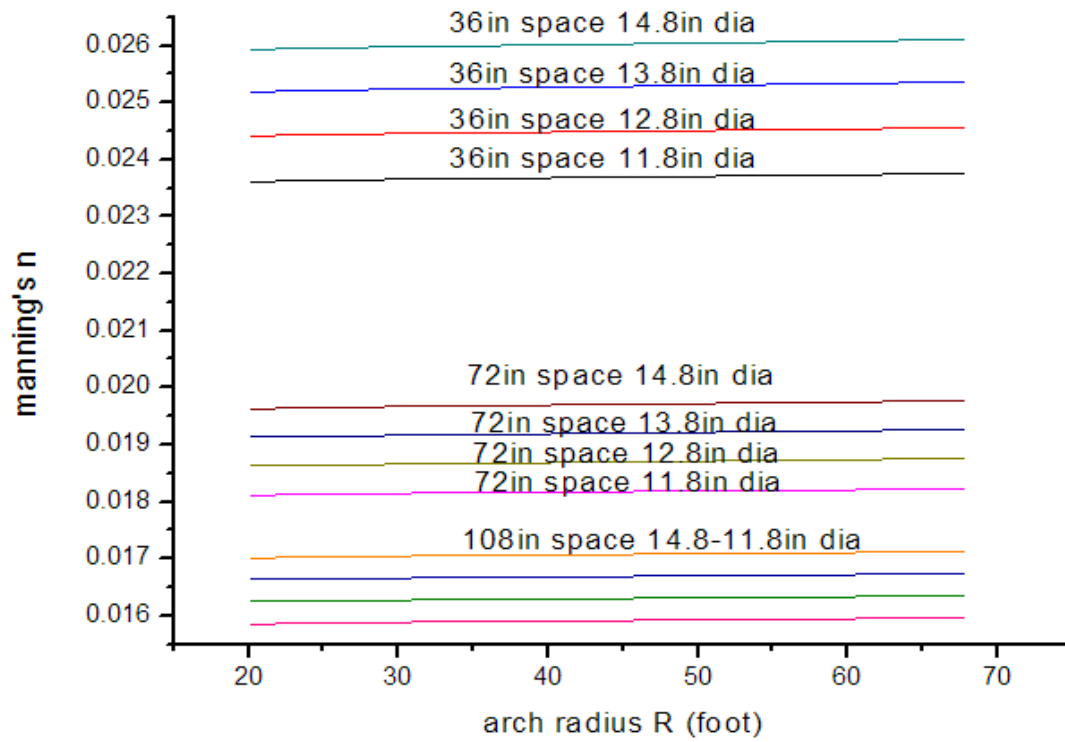


Figure 21: Manning's coefficient with arch radius R (Flow angle: 45 degrees).

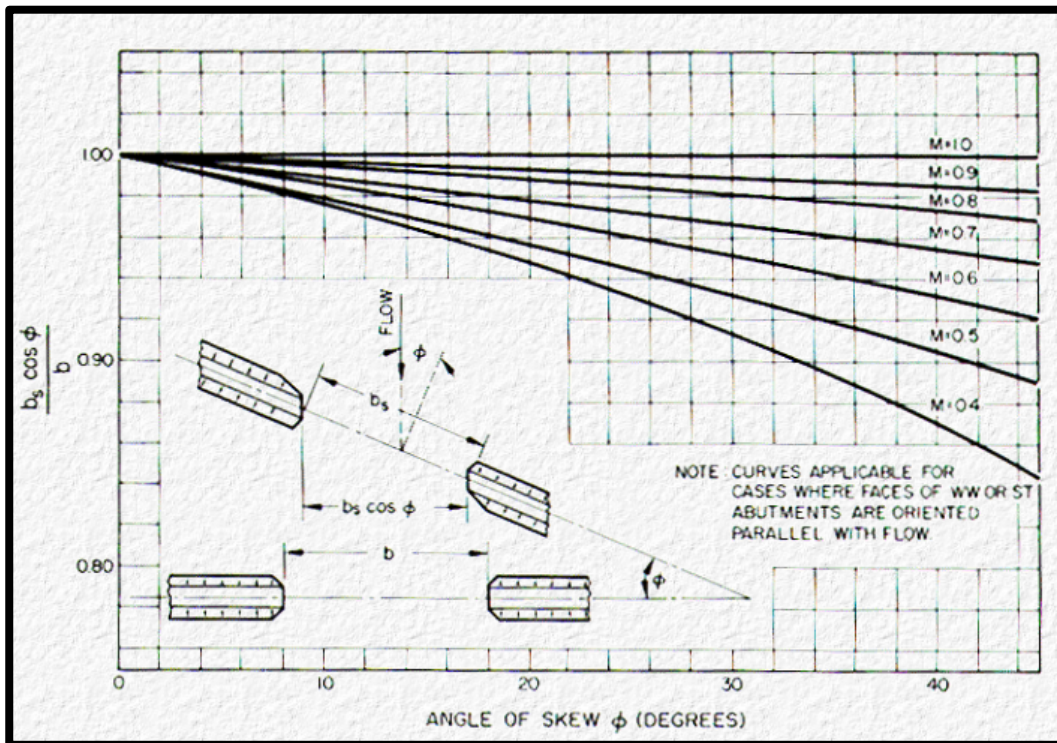


Figure 22: Ratio of projected to normal length of bridge for equivalent backwater (Skewed crossings [19]).

In bridge waterways skewed bridge crossings are generally handled by making adjustments to the bridge dimensions to define an equivalent cross section perpendicular to the flow line [19]. The method is shown in Figure 19. In the figure, M is bridge opening ratio, which defines the degree of stream constriction involved, expressed as the ratio of the flow that can pass unimpeded through the bridge constriction to the total flow of the river. An option called Skew Bridge/Culvert is available from the bridge/culvert editor in HEC-RAS.

5. CONCLUSIONS

The results show when the flow is perpendicular to the buried composite arch bridge, the design state could be in either hyper turbulent or isolated roughness flow regime. Manning's n is related to radius of arch, tube diameter and tube spacing. Manning's coefficient has to be evaluated differently at different flow regimes. The conventional method of deriving Manning's coefficient is not valid for this technology due to the large tube space and size. We used the formula for hyper turbulent flow when tubes are sufficiently close so each tube is in the wake of the previous tube and rough surface vortices are the primary source of the overall friction drag. We used the formula for isolated roughness flow when tube spacing is large and overall resistance is due to drag on the culvert surface plus form drag on the tube.

The overall flow resistance, Manning's roughness coefficient, decreases as the relative spacing of tubes (ratio of tube spacing to size) increases at the isolated-roughness flow regime, whereas it increases with the relative spacing of roughness at the hyper turbulent flow regime. Our study shows that when the tube spacing, L is small, the Manning's n decreases with the arch radius R (Figure 15). But when the tube spacing L is large, the Manning's n is hardly affected by the arch radius R , but is by the diameter of tube. Depending on the arch radius and tube size and spacing, Manning's roughness coefficient of the bridge ranges from 0.016 to 0.045, which is significantly larger than that for smooth concrete at $n=0.012$, due to the large tubes underneath the bridge. These results are important findings and should be incorporated in a hydraulic model such as HECRAS to more accurately predict water flows and backwater profile at the FRP tubular bridge.

The Manning roughness coefficient decreases with the increasing angle of attack of the flow relative to the bridge. When the angle of flow and bridge is 45 and 30 degrees and flow speed reaches the value in Table 5, the flow is in isolated roughness flow. If the flow velocity lies in between the laminar velocity and velocity in Table 5, interpolation can be used to obtain Manning's n .

6. REFERENCES

- [1] Habib J. Dagher, Daniel J. Bannon, William G. Davids, Lopez-Anido, E. A., Nagy, E. Goslin K. (2012). Bending behavior of concrete-filled tubular FRP arches for bridge structures. *Construction and Building Materials* 37. 432-439.
- [2] Bannon, D.J. (2009). Characterization of Concrete-Filled Fiber-Reinforced Polymer Arch Members. Master's Thesis, Dept. of Civil and Environmental Engineering, University of Maine.
- [3] Nagy, Edwin, et al (2009). Design, Construction, and Testing of the Neal Bridge in Pittsfield, Maine – Final Report, University of Maine, Orono, Maine. Technical Report to Maine DOT.
- [4] Stephen T. Maynard.(1989). RIPRAP DESIGN. *J. Hydraul. Eng.* 115:937-949.
- [5] S. He and C. Ariyaratne (2011). Wall Shear Stress in the Early Stage of Unsteady Turbulent Pipe Flow. *JOURNAL OF HYDRAULIC ENGINEERING* , 606-611.
- [6] Stefano Pagliara and Iacopo Carnacina (2011). Influence of Wood Debris Accumulation on Bridge Pier Scour. *JOURNAL OF HYDRAULIC ENGINEERING*, pp.254-262
- [7] B. Mottahed (1996). Artificial roughness effects on turbulent transfer coefficients in the entrance region of a circle tube. *Int. J. Heat Mass Transfer*. Vol. 39, No. 12. pp.2515-2523.
- [8] Corps of Engineers (1987). Hydraulic design criteria. SHEETS 224-1/5 AND 224-1/6.
- [9] Terry W. Sturm (2001). Open Channel Hydraulics. McGraw Hill, pp97-142.
- [10] U.S. Army Corps of Engineers (2010). HEC-RAS River Analysis System. User's Manual. Version 4.1.
- [11] U.S. Department of Transportation (2012). Hydraulic Engineering Circular No. 14, Third Edition. Hydraulic Design of Energy Dissipators for Culverts and Channels. National Highway Institute.
- [12] Morris, H. M., (1963). Applied Hydraulics In Engineering, The Ronald Press Company, New York.
- [13] Wiggert, J. M. and P. D. Erfle (1971). Roughness Elements as Energy Dissipators of Free Surface Flow in Circular Pipes, HPR #373, pp. 64-73, TRB, Washington, D.C.

- [14] ACPA, (1972). Culvert Velocity Reduction by Internal Energy Dissipators, Concrete Pipe News, pp. 87-94, American Concrete Pipe Association, Arlington, VA.
- [15] Henry M. Morris, James M. Wiggert (1971). Applied Hydraulics in Engineering (2nd). Ronald.
- [16] Bursnall, William J. Loftin and Laurence K. (1951). Experimental investigation of the pressure distribution about a yawed circular cylinder in the critical Reynolds number range. NASA TN 2462.
- [17] Smith, R.A, Moon, Woo (1972), Taik. Experiments on flow about a yawed circular cylinder. *Journal of Basic Engineering*.
- [18] Edward C. Polhamous. A review of some Reynolds number effects related to bodies at high angles of attack. NASA Contractor Report 3809.
- [19] Joseph N. Bradley (1978), FHWA, Bridge Division. Hydraulics of Bridge Waterways HDS 1.

Appendix 1 Table of Roughness Coefficient (Manning's n)

Table A1 Flow perpendicular to bridge

Radius of arch	R=20.22ft				R=23.46ft				R=67.87ft			
Tube spacing	d=11.8in	12.8in	13.8in	14.8in	d=11.8in	12.8in	13.8in	14.8in	d=11.8in	12.8in	13.8in	14.8in
30	0.038	0.038	0.038	0.038	0.038	0.038	0.038	0.038	0.036	0.036	0.036	0.036
36	0.040	0.040	0.040	0.040	0.040	0.040	0.040	0.040	0.037	0.037	0.037	0.037
42	0.042	0.042	0.042	0.042	0.041	0.041	0.041	0.041	0.039	0.039	0.039	0.039
48	0.043	0.043	0.044	0.044	0.043	0.043	0.043	0.043	0.040	0.040	0.040	0.040
54	0.043	0.044	0.045	0.045	0.043	0.044	0.044	0.044	0.041	0.041	0.041	0.041
60	0.041	0.042	0.044	0.045	0.041	0.042	0.044	0.045	0.041	0.042	0.042	0.042
66	0.039	0.040	0.042	0.043	0.039	0.040	0.042	0.043	0.039	0.041	0.042	0.043
72	0.037	0.039	0.040	0.041	0.037	0.039	0.040	0.042	0.038	0.039	0.040	0.042
78	0.036	0.037	0.039	0.040	0.036	0.037	0.039	0.040	0.036	0.038	0.039	0.040
84	0.035	0.036	0.037	0.039	0.035	0.036	0.037	0.039	0.035	0.036	0.038	0.039
90	0.034	0.035	0.036	0.037	0.034	0.035	0.036	0.037	0.034	0.035	0.036	0.038
96	0.033	0.034	0.035	0.036	0.033	0.034	0.035	0.036	0.033	0.034	0.035	0.037
102	0.032	0.033	0.034	0.035	0.032	0.033	0.034	0.035	0.032	0.033	0.034	0.036
108	0.031	0.032	0.033	0.034	0.031	0.032	0.033	0.034	0.031	0.032	0.034	0.035

d: diameter of tube

Table A2 Angle of flow and bridge is 45 degrees.

Radius of arch	R=20.22ft				R=23.46ft				R=67.87ft			
Tube spacing	d=11.8in	12.8in	13.8in	14.8in	d=11.8in	12.8in	13.8in	14.8in	d=11.8in	12.8in	13.8in	14.8in
30	0.025	0.026	0.027	0.028	0.026	0.026	0.027	0.028	0.026	0.027	0.027	0.028
36	0.024	0.024	0.025	0.026	0.024	0.024	0.025	0.026	0.024	0.025	0.025	0.026
42	0.022	0.023	0.024	0.024	0.022	0.023	0.024	0.024	0.022	0.023	0.024	0.024
48	0.021	0.022	0.022	0.023	0.021	0.022	0.022	0.023	0.021	0.022	0.023	0.023
54	0.020	0.021	0.021	0.022	0.020	0.021	0.021	0.022	0.020	0.021	0.021	0.022
60	0.019	0.020	0.020	0.021	0.019	0.020	0.021	0.021	0.019	0.020	0.021	0.021
66	0.019	0.019	0.020	0.020	0.019	0.019	0.020	0.020	0.019	0.019	0.020	0.020
72	0.018	0.019	0.019	0.020	0.018	0.019	0.019	0.020	0.018	0.019	0.019	0.020
78	0.018	0.018	0.019	0.019	0.018	0.018	0.019	0.019	0.018	0.018	0.019	0.019
84	0.017	0.018	0.018	0.019	0.017	0.018	0.018	0.019	0.017	0.018	0.018	0.019
90	0.017	0.017	0.018	0.018	0.017	0.017	0.018	0.018	0.017	0.017	0.018	0.018
96	0.016	0.017	0.017	0.018	0.016	0.017	0.017	0.018	0.017	0.017	0.017	0.018
102	0.016	0.017	0.017	0.017	0.016	0.017	0.017	0.017	0.016	0.017	0.017	0.017
108	0.016	0.016	0.017	0.017	0.016	0.016	0.017	0.017	0.016	0.016	0.017	0.017

d: diameter of tube

Table A3 Angle of flow and bridge is 30 degrees.

Radius of arch	R=20.22ft				R=23.46ft				R=67.87ft			
Tube spacing	d=11.8in	12.8in	13.8in	14.8in	d=11.8in	12.8in	13.8in	14.8in	d=11.8in	12.8in	13.8in	14.8in
30	0.0278	0.0288	0.0298	0.0307	0.0279	0.0289	0.0298	0.0307	0.0280	0.0290	0.0300	0.0309
36	0.0257	0.0266	0.0275	0.0283	0.0258	0.0266	0.0275	0.0283	0.0259	0.0268	0.0277	0.0285
42	0.0241	0.0249	0.0257	0.0265	0.0241	0.0250	0.0257	0.0265	0.0242	0.0251	0.0259	0.0267
48	0.0228	0.0236	0.0243	0.0250	0.0228	0.0236	0.0243	0.0250	0.0230	0.0237	0.0245	0.0252
54	0.0218	0.0225	0.0232	0.0238	0.0218	0.0225	0.0232	0.0238	0.0219	0.0226	0.0233	0.0240
60	0.0209	0.0215	0.0222	0.0228	0.0209	0.0216	0.0222	0.0228	0.0210	0.0217	0.0223	0.0230
66	0.0201	0.0208	0.0214	0.0219	0.0202	0.0208	0.0214	0.0220	0.0203	0.0209	0.0215	0.0221
72	0.0195	0.0201	0.0207	0.0212	0.0195	0.0201	0.0207	0.0212	0.0196	0.0202	0.0208	0.0214
78	0.0189	0.0195	0.0200	0.0206	0.0190	0.0195	0.0201	0.0206	0.0190	0.0196	0.0202	0.0207
84	0.0184	0.0190	0.0195	0.0200	0.0185	0.0190	0.0195	0.0200	0.0185	0.0191	0.0196	0.0201
90	0.0180	0.0185	0.0190	0.0195	0.0180	0.0185	0.0190	0.0195	0.0181	0.0186	0.0191	0.0196
96	0.0176	0.0181	0.0186	0.0190	0.0176	0.0181	0.0186	0.0190	0.0177	0.0182	0.0187	0.0192
102	0.0172	0.0177	0.0182	0.0186	0.0173	0.0177	0.0182	0.0186	0.0173	0.0178	0.0183	0.0187
108	0.0169	0.0174	0.0178	0.0182	0.0169	0.0174	0.0178	0.0183	0.0170	0.0175	0.0179	0.0184

d: diameter of tube

Appendix 2 Feasibility Study of Physical Test in UMaine Flume

Quasi-smooth flow is complex. The coefficient of Manning's n for this type of flow should be confirmed in model test. We planned a model test at a scale of 1:70.4 according to the dimensions of the lab. The total length and width of flumes is 4 meters and 1 foot, respectively; the maximum achievable scale is 1:70.4.

Based on Chézy formula and Manning formula as in reference [1*]

$$v = C\sqrt{RJ} \quad (\text{A-1})$$

$$v = \frac{1}{n} R^{2/3} J^{1/2} \quad (\text{A-2})$$

Where J is Hydraulic gradient, C is coefficient of Chézy, and R is hydraulic radius.

For uniform turbulent flow, frictional head loss is

$$h_f = f \frac{L}{4R} \frac{v^2}{2g} \quad (\text{A-3})$$

Where f is Darcy's f , L is distance between 2 observation section. R is hydraulic radius. V is average flow velocity of section. G is acceleration of gravity.

So,

$$f = \frac{8gRh_f}{v^2L} \quad (\text{A-4})$$

$$C = \frac{1}{n} R^{1/6} \quad (\text{A-5})$$

$$n = R^{1/6} \sqrt{\frac{f}{8g}} \quad (\text{A-6})$$

$$h_f = \frac{n^2Lv^2}{R^{4/3}} \quad (\text{A-7})$$

Considering the link section, the maximum length to be used is about 3 meters. We aim to get a 10 cm water head loss, which is a classic experience value in hydraulics test as in reference [2*]. Based on the calculated result the Manning's n is 0.02 in model test. If the arch radius in prototype is 23.46 ft, the corresponding arch radius in mode test is 0.21meter. So the velocity must reach as high as,

$$v^2 = \frac{h_f R^{4/3}}{n^2 L} = \frac{0.1 * (\frac{0.21}{2})^{4/3}}{0.02^2 * 3.0} = 2.03 m/s$$

The flume in the lab is not capable of this velocity. It appears unfeasible to perform meaningful experiments in the lab for this project.

References

- [1*] Terry W. Sturm. Open Channel Hydraulics. McGraw Hill. 2001, pp. 97-142.
- [2*] Yangtze River Scientific Research Institute. Hydraulics prototype observation in hydraulic structure. Chinese water resource and hydraulic press. 1988.